


FEATURED ARTICLE

APP accumulates with presynaptic proteins around amyloid plaques: A role for presynaptic mechanisms in Alzheimer's disease?

Tomàs Jordà-Siquier¹ | Melina Petrel² | Vladimir Kouskoff¹ | Una Smailovic³ |
Fabrice Cordelières² | Susanne Frykman³ | Ulrike Müller⁴ | Christophe Mulle¹ |
Gaël Barthet¹ 

¹ University Bordeaux, CNRS, Interdisciplinary Institute for Neuroscience, IINS, UMR 5297, Bordeaux, France

² University Bordeaux, CNRS, INSERM, Bordeaux Imaging Center, BIC, UMS 3420, US 4, Bordeaux, France

³ Division of Neurogeriatrics, Center for Alzheimer Research, Department of Neurobiology, Care Sciences and Society, Karolinska Institutet, Solna, Sweden

⁴ Institute for Pharmacy and Molecular Biotechnology, Heidelberg, Germany

Correspondence

Gaël Barthet, University Bordeaux, CNRS, Interdisciplinary Institute for Neuroscience, IINS, UMR 5297, Bordeaux F-33000, France.
Email: gael.barthet@u-bordeaux.fr

Funding information

European Union's Horizon 2020 research and innovation program, Grant/Award Number: 676144; Fondation pour la Recherche Médicale, Grant/Award Number: #DEQ20160334900

Abstract

In Alzheimer's disease (AD), the distribution of the amyloid precursor protein (APP) and its fragments other than amyloid beta, has not been fully characterized. Here, we investigate the distribution of APP and its fragments in human AD brain samples and in mouse models of AD in reference to its proteases, synaptic proteins, and histopathological features characteristic of the AD brain, by combining an extensive set of histological and analytical tools. We report that the prominent somatic distribution of APP observed in control patients remarkably vanishes in human AD patients to the benefit of dense accumulations of extra-somatic APP, which surround dense-core amyloid plaques enriched in APP-Nter. These features are accentuated in patients with familial forms of the disease. Importantly, APP accumulations are enriched in phosphorylated tau and presynaptic proteins whereas they are depleted of post-synaptic proteins suggesting that the extra-somatic accumulations of APP are of presynaptic origin. Ultrastructural analyses unveil that APP concentrates in autophagosomes and in multivesicular bodies together with presynaptic vesicle proteins. Altogether, alteration of APP distribution and its accumulation together with presynaptic proteins around dense-core amyloid plaques is a key histopathological feature in AD, lending support to the notion that presynaptic failure is a strong physiopathological component of AD.

KEYWORDS

Alzheimer's disease, amyloid, amyloid precursor protein, presynaptic proteins, protein accumulation

This is an open access article under the terms of the [Creative Commons Attribution-NonCommercial-NoDerivs](https://creativecommons.org/licenses/by-nc-nd/4.0/) License, which permits use and distribution in any medium, provided the original work is properly cited, the use is non-commercial and no modifications or adaptations are made.

© 2022 The Authors. *Alzheimer's & Dementia* published by Wiley Periodicals LLC on behalf of Alzheimer's Association

1 | NARRATIVE

1.1 | Contextual background

Despite important breakthroughs in the genetic and in the cellular biology of Alzheimer's disease (AD) pathology, the etiology of the disease is still unknown. Compelling neuropathological and genetic evidence^{1–3} support the amyloid cascade hypothesis,⁴ which postulates that the neurodegeneration in AD is caused by abnormal build-up of amyloid beta (A β) plaques in various areas of the brain. However, until very recently, all clinical trials based on this theory have repetitively failed to halt or to delay AD progression.^{5,6} Lately, an anti-amyloid antibody has been approved for medical use after showing moderate but controversial efficacy.⁷ There is thus a strong need for alternative hypotheses to explain AD pathology and to design new therapeutic interventions. Here, we provide early evidence supporting such an alternative hypothesis of a role for the amyloid precursor protein (APP) as a local substrate for plaque formation and of presynaptic protein impairment in AD pathology.

The central role attributed to A β peptides, a by-product of APP degradation, contrasts with the mechanisms involved in most other neurodegenerative diseases in which full-length (misfolded) proteins aggregate and accumulate inside neurons.^{8,9} However, several pieces of genetic evidence support the idea that excess APP itself is toxic for neurons. Down syndrome patients, who have three copies of the APP gene,^{10–12} as well as patients with a rare APP gene duplication,^{13,14} suffer from early forms of AD. Moreover, apolipoprotein E ϵ 4, the main genetic risk factor of AD, markedly promotes APP expression.¹⁵ Finally, presenilin 1 (PS1) FAD (familial AD) mutations impair the cleavage of APP by PS^{16–19} leading to the accumulation of uncleaved substrates potentially toxic for the cell as a result of impaired catabolism.^{20–24} However, this array of genetic evidence has been systematically used in favor of a role of A β peptides instead of a direct role of APP. Indeed, APP being the precursor of A β , an excess of APP could lead to excess A β production and plaque formation.

Clinical and neuropathological studies have long indicated that synaptic impairment correlates strongly with the cognitive deficits seen in AD.^{25–28} Moreover, evidence for alterations specific to the presynaptic compartment in AD has recently grown. For example, we have reported that deletion of presenilin, the protease responsible for the production of A β peptide from APP cleavage, markedly decreases the abundance of synaptotagmin-7, a key calcium sensor involved in presynaptic plasticity.²⁹ We and others have also reported downregulation of presynaptic proteins in AD brains^{30–32} including proteins determinant of cognitive reserve like complexin-1.^{33,34} This collection of data has led us to advocate for the hypothesis of presynaptic failure in AD.³⁵ This hypothesis stipulates that the initial pathological mechanism in AD involves a strong presynaptic component.

Limited information is available about the distribution and the abundance of full-length APP, and its fragments other than A β , in the human AD brain. The presence of neuritic accumulations of APP in AD brains was reported in early studies.^{36,37} However, a thorough analysis of the distribution of the different APP fragments other than A β within and

RESEARCH IN CONTEXT

- 1. Systematic Review:** The authors searched PubMed using the terms “Alzheimer disease,” “APP,” “distribution.” The presence of neuritic accumulations of amyloid precursor protein (APP) in Alzheimer's disease (AD) brains was reported in early studies. However, a thorough analysis of the distribution of the different APP fragments other than amyloid beta, within and outside neurons, between sporadic and familial AD, and a detailed molecular characterization of the compartments where APP accumulates are still missing.
- 2. Interpretation:** Our study highlights APP misdistribution from the soma to impaired presynaptic sites in AD pathology and suggests presynaptic APP accumulations as potential substrates to supply dense-core plaques with amyloid peptides and APP-Nter. The heavier burden in the early-onset, familial form of AD suggests a role of APP accumulation in the faster progression of the disease.
- 3. Future Directions:** In vivo microscopy in animal models with APP and presynaptic proteins tagged with a fluorescent protein will help to decipher the cause–consequence relationship between presynaptic APP accumulation and plaque formation. Going forward, preclinical studies will address the potential relevance of therapeutic intervention against APP-Nter.

outside neurons, in sporadic and familial AD, and a detailed molecular characterization of the compartments where APP accumulates are still missing. Here, we aimed at investigating APP-related proteinopathy in human brain samples with regard to presynaptic proteins, APP proteases, and histopathological features of the AD brain.

1.2 | Study design and main results

We combined triple-immunofluorescence labeling and electron microscopy (EM) in hippocampal sections from a cohort of 27 human patients and from the APP/PS1 and APP-NL/G/F mouse models of AD aiming to address the distribution of APP and its fragments in an unbiased approach. We compared the distribution of APP in the human hippocampus of AD cases versus controls, by collecting paraffin-embedded hippocampal sections from two brain banks: the Netherlands Brain Bank (NBB) and the Karolinska Institutet Brain Bank (KIBB) (see Methods). Three groups were constituted: 11 controls patients (mean age 79.6 years; 73% F and 27% M), 12 sporadic AD patients (mean age 81 years; 92% F and 8% M), and 4 FAD patients (mean age: 48.5 years; 50% F and 50% M; summarized in Table 1; detailed clinical data tables in Table S1–S3 in supporting information).

We performed a detailed characterization of the distribution of APP fragments in the human AD hippocampus. We report that the

TABLE 1 Clinical resume table

Case	Sex	Braak stage	Age of onset	Age of death	PMD (h)	Brain weight (g)	CSF pH	Brain bank	Number of patients
Control	F/M (73/27%)	I-III	-	79.6	8.54	1204	6.75	NBB/KI	11
SAD	F/M (92/8%)	V-VI	72.1	81	11.08	1061	6.43	NBB/KI	12
FAD	F/M (50/50%)	V-VI	40.7	40.7	3.5	1101	6.22	NBB/KI	4

Abbreviations: CSF, cerebrospinal fluid; F, female; FAD, familial Alzheimer's disease; KI, Karolinska Institute; M, male; NBB, Netherlands Brain Bank; PMD, post-mortem delay; SAD, sporadic Alzheimer's disease.

prominent distribution of APP in neuronal soma observed in control brains is markedly decreased in the AD condition. On the contrary, we observed extra-somatic microscopic entities of remarkably intense APP stainings in AD cases (enrichment by a factor 9). APP, together with β - and γ -secretases, preferentially accumulates around dense-core amyloid plaques enriched in APP-Nter (enrichment by a factor 2.3), but not in APP-Cter domain. The subcellular compartment in which APP concentrates is enriched in presynaptic proteins and is conversely depleted in post-synaptic proteins. In addition, APP accumulations are more abundant in FAD patients bearing PS1 mutations suggesting that the accumulations relate to impaired APP proteolysis, and finally their abundance correlates with neuronal loss in AD mouse models.

1.3 | Study conclusions, disease implications, and therapeutic opportunities

The observation of APP accumulations together with APP-proteases and presynaptic proteins around dense-core plaques containing APP-Nter has potentially important consequences for AD pathology paradigms. The classical paradigm of amyloid plaque formation proposes that A β peptides, ubiquitously produced in the brain and in the periphery, would circulate in extracellular fluids before seeding and aggregating within amyloid plaques.^{38,39} However, this rationale seems inconsistent with the long-observed decrease of A β concentration in cerebrospinal fluid and plasma of AD patients compared to non-demented controls.⁴⁰ One of the alternative paradigms of amyloid plaque formation, formulated by Fisher in 1907 in his early description of AD pathology, proposes that amyloid plaques derive from dystrophic, degenerating neuronal processes (reviewed in Gouras et al.⁴¹). Our report that cellular structures, enriched in both APP and APP-proteases, surround amyloid plaques enriched not only in A β peptide but also in APP-Nter (see Figures 1–3), advocates that APP accumulations represent a local source for A β and APP-Nter peptides composing the dense-core plaques. Indeed, the localization in the same compartments of APP and its secretases favors enzyme–substrate collisions and therefore APP processing. This alternative mechanism for the formation of A β plaques is also supported by the remarkable correlation between APP accumulations and amyloid plaques areas.

Interestingly, the number of APP accumulations is higher in patients with a genetically inherited, early-onset form of AD (FAD cases; Figure 1D and S1F) whereas this group does not present higher tau

or amyloid Braak stages compared to the sporadic AD (SAD) cohort (Tables S2 and S3). Finally, we observed an inverse correlation between the number of APP accumulations and neuronal density in a mouse model of AD (see Figure 6). This suggests a role of APP accumulations in AD pathology that should be further investigated in future studies.

In addition to their potential pathogenic role as local sources to fuel amyloid plaques described above, APP accumulations may also trigger degeneration through impairing presynaptic function. APP interacts with several proteins of the synaptic release machinery,⁴² raising the possibility that its accumulation in pathological conditions leads to co-aggregation or misrouting of synaptic vesicle proteins,²⁹ which are not only essential to presynaptic function but also to neuronal survival. Indeed, the genetic deletion, or the loss of function of several presynaptic proteins (e.g., Munc18, α -synuclein, syntaxin1, or SNAP-25) leads to neurodegeneration.^{43–46} Our observation of the selective accumulation of presynaptic proteins in APP accumulations contrasts with recent discoveries from us and others of broad downregulation of presynaptic proteins in AD brains^{29–32} and indicates that the alteration of presynaptic proteins in AD is spatially heterogeneous. In the AD hippocampus, APP follows a complex pattern of misdistribution, too, accumulating within neuropil areas, and vanishing in neuronal somata where APP is normally prominent. Importantly, the decrease in somatic APP in neurons correlates with the extent of APP accumulations burden in the neuropil, suggesting that the two phenomena are linked. An impairment of axonal transport represents a simple and straightforward explanation for such a misdistribution of APP and presynaptic proteins in the AD brain. A traffic jam would lead, on one hand, to the pathological accumulation of proteins at the site of blockage, and on the other hand, to their deficit where they exert their physiological function.

The presence of multi-vesicular bodies harboring presynaptic vesicle proteins in APP accumulations may represent the endpoint of an axonal degeneration process. Indeed, APP accumulation is a marker of axonal damage in several pathologies including multiple sclerosis,^{47,48} myelopathy,⁴⁹ herpes simplex encephalitis,⁵⁰ or even traumatic brain injury.^{51,52} Given the well-established fast axonal transport of APP,^{53,54} APP may accumulate in AD as a result of axonal injury. Destabilization of axonal microtubules by alterations (e.g., over-phosphorylation) of the microtubule-stabilizing protein tau,⁵⁵ which is enriched within APP accumulations, is a possible mechanism for axonal injury. Along these lines, deletion of tau reduces BACE1 around plaques and slows plaque formation in an AD mouse model.⁵⁶ Together, our

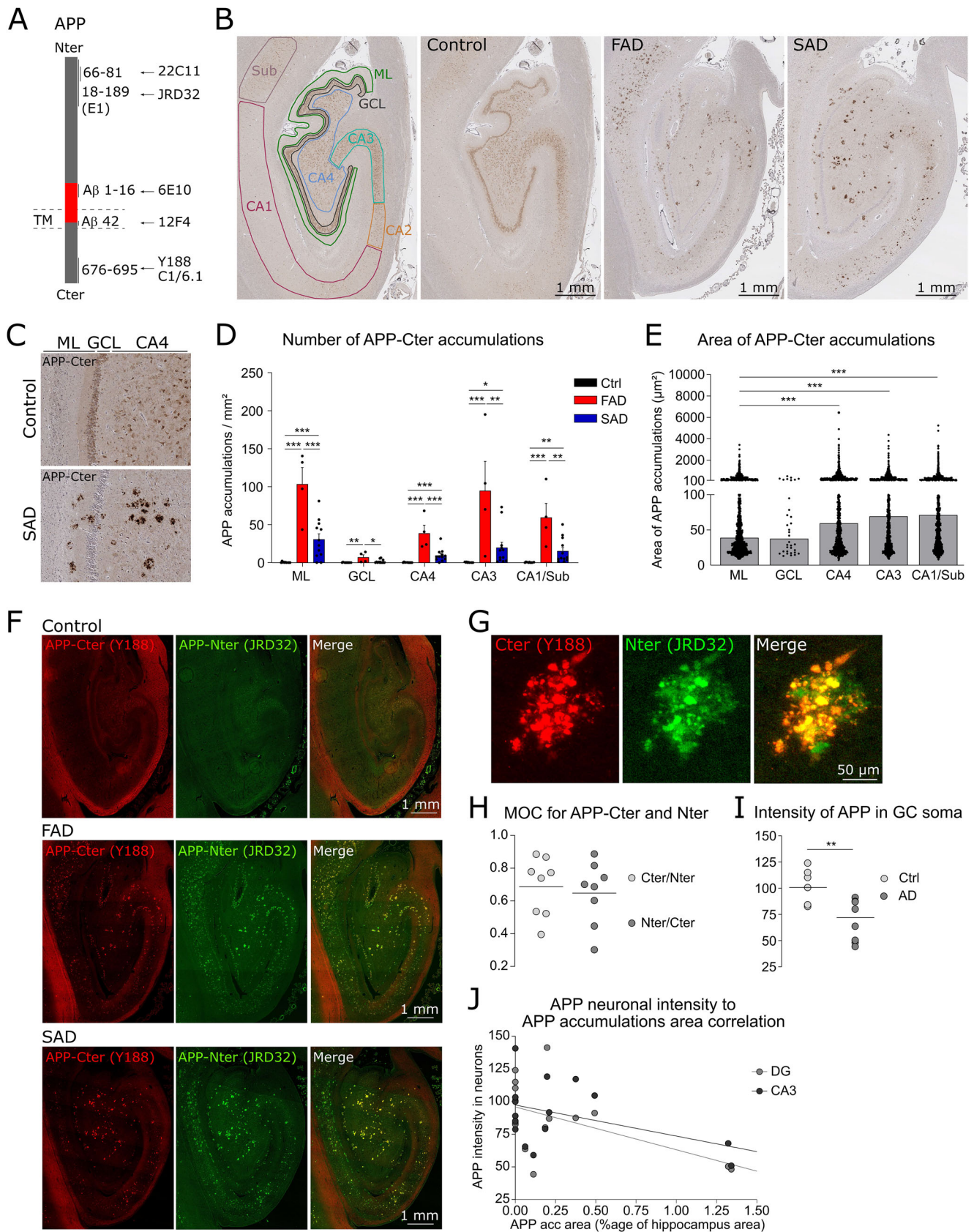


FIGURE 1 APP misdistribution in the hippocampus of AD patients (A) Scheme of full-length APP showing the epitopes in the Nter, Cter and A β domains of six antibodies against APP. The red segment represents the A β sequence spanning through the transmembrane (TM) domain. (B) Pictures of human hippocampal sections stained by DAB against APP-Cter with C1/6.1 antibody. Cases from control, FAD and SAD groups are illustrated. The first panel on the left depicts different anatomical regions where the subsequent quantifications have been performed. In controls,

results support a role of presynaptic APP in AD pathology, within phosphorylated tau (p-tau)-positive dystrophic axons, where synaptic vesicle proteins are misdistributed, in keeping with a presynaptic failure hypothesis.⁵⁷

Whatever the mechanisms involved in APP pathological function (local source to fuel amyloid plaques, primer of presynaptic failure, etc.), targeting APP in AD therapeutic trials could be promising. Indeed, despite numerous clinical trials targeting the A β peptide (β -secretase or γ -secretase inhibitors, active or passive immunotherapy against A β peptides), no treatment to cure or even to slow down AD progression is available.^{5,6} As an alternative approach, we propose the Nter domain of APP, very accessible to the binding of therapeutic molecules due to its extracellular topology, as a therapeutic target in an attempt to prevent APP accumulation and misprocessing. Other promising therapeutic strategies consist in protecting the axon integrity (by targeting the microtubules, or their associated proteins or enzymes) or in targeting synaptic proteins involved in plasticity and in cognitive reserve like complexin-1.

1.4 | Limitations, unanswered questions, and future directions

The use of *post mortem* brain tissue from AD patients allows a detailed molecular characterization of histopathological features in humans but comes with substantial limitations. Mainly, the inherent nature of the fixed tissue does not allow testing of the sequence of pathological events. However, the resolution of the cause-consequence relationship among APP accumulation, presynaptic proteins impairment and amyloid plaques formation, and the discovery of their role in neuronal loss will answer the complex question whether the therapeutic attempt to cure AD must continue to target A β peptides or not. If in AD, protein accumulation starts with APP and presynaptic proteins, then amyloid plaques might just be the endpoint of a cascade of protein-related pathological events. In such a case, it is not surprising that amyloid-targeting immunotherapies have failed to show strong clinical efficacy despite an efficacious clearing of amyloid plaques.⁵⁸

We report here that amyloid mouse models (APP/PS1 and APP-KI NL/G/F) recapitulate the APP-related features we have observed in human samples (see Figure 5). Time-lapse experiments using two-photon microscopy in AD mouse models has been demonstrated to be highly relevant for following the kinetics of pathological events.⁵⁹ The injection of AD mouse models with viruses expressing fluorescently tagged APP in the entorhinal cortex (EC) will allow us to follow the appearance of presynaptic APP accumulations in the hippocampus where the axons form EC neurons project and to test whether the APP accumulations precede the formation of amyloid plaques observed with methoxy-X04.

Similarly, video tracking of fluorescently tagged presynaptic proteins will allow us to interrogate why and how accumulations of presynaptic proteins are formed with respect to the traffic jam hypothesis. For example, investigation of axonal integrity (microtubules, neurofilaments, and actin skeletons) in relationship with axonal pathology (APP and presynaptic accumulations) will shed light on the early molecular mechanisms of AD. It will address the order of appearance of presynaptic protein accumulations, amyloid plaques, and cognitive impairments. Misdistribution of presynaptic proteins could constitute one of the earliest events in the pathological process; it could significantly contribute to dysfunctional information processing and to the impairment of cognition observed in AD before massive neuronal death occurs. For example, misdistribution of presynaptic proteins could lead to the reduction of functional synapses, and/or alteration of synaptic strength or synaptic plasticity. The exploration of the mechanisms involved in synaptic dysfunction could thus provide a new generation of therapeutic targets to prevent synapse loss and treat neurodegeneration in AD.

2 | CONSOLIDATED RESULTS AND STUDY DESIGN

Here we carried out 3,3'-diaminobenzidine (DAB) staining or triple-immunofluorescence labeling of APP fragments together with synaptic or AD-related markers in a cohort of 27 human patients and in the

APP is stained mostly in the soma of neuronal layers of the dentate gyrus granule cells (GCL), CA4 and CA3. In both FAD and SAD cases, intense extrasomatic APP stainings are observable. (C) Image magnification of the dentate gyrus as in 'B'. In the SAD case, intense extra-somatic APP accumulations are observable in the dentate gyrus molecular layer (ML), GC and CA4 regions. (D) Histogram of the number of APP-Cter accumulations in different hippocampal regions in the control (ctrl), FAD or SAD conditions. APP accumulations are barely detected in Ctrl whereas they are abundant in AD. The number of accumulations is higher in FAD compared to SAD condition. (E) Histogram of the area of APP accumulations in different hippocampal regions. The CA regions contain larger APP accumulations than the ML. (F) Human hippocampal sections fluorescently immuno-labeled against APP-Cter with Y188 antibody and APP-Nter with JRD32. In controls, both Cter and Nter APP antibodies mostly label the soma of neurons in the GCL, CA4 and CA3. In addition, Y188 nonspecifically stained the white matter tracts (see FigS1C). In both FAD and SAD cases, intense extra-somatic APP stainings, co-labeled with the two antibodies are observable. (G) Close-up picture of an APP accumulations co-labeled with APP-Cter and Nter antibodies. (H) Scatter plot of Manders overlapping coefficients (MOC) (Method described in FigS1L-M) between APP-Cter and Nter labelings. The analysis revealed a high colocalization between the two channels suggesting the presence of full-length APP in the accumulations. (I) Scatter plot of the intensity of APP labelling in the GC soma normalized to the mean intensity in controls. The intensity is significantly reduced in the AD group (J) Graph of the mean pixel intensity of APP staining in neuronal somas in function of the area covered by APP accumulations (normalized to the hippocampus area). The linear regression of the data presents a negative slope. The Pearson correlation coefficient was -0.53 for DG ($p = 0.035$), -0.43 for CA3 ($p = 0.046$), indicative of an inverse correlation between the extent of APP accumulations and APP intensity in the neuronal soma

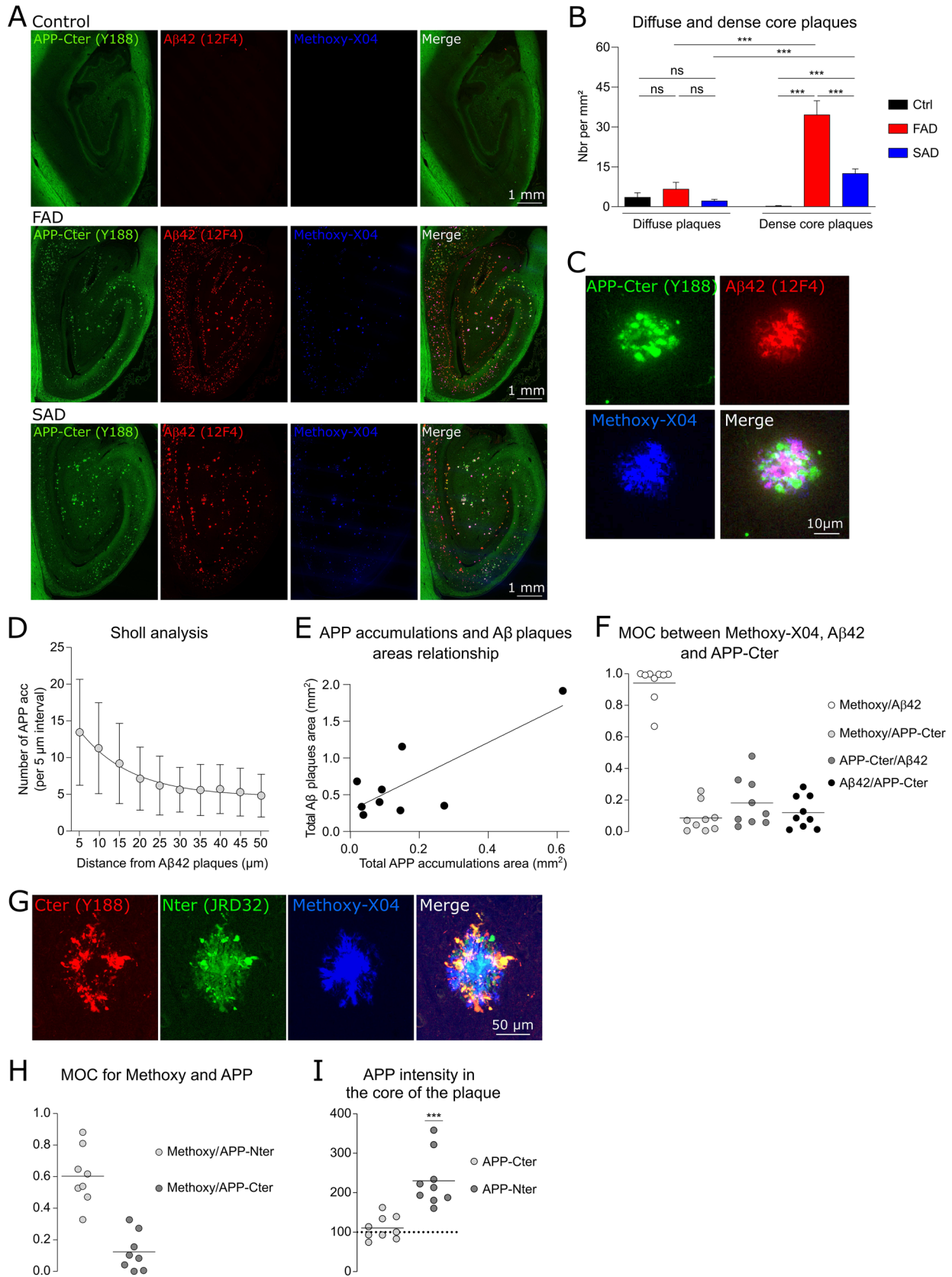


FIGURE 2 APP accumulations surround dense-core amyloid plaques enriched in APP-Nter (A) Human hippocampal sections fluorescently immuno-labeled against APP-Cter and A β 42 with respectively Y188 and 12F4 antibodies and with methoxy-X04. In both FAD and SAD cases, intense A β 42 and methoxy-X04 labelings are observable in close proximity to APP accumulations whereas no staining is observable in control. (B) Histogram of the density of diffuse and dense core plaque in the hippocampus in the control (ctrl), FAD or SAD conditions. Moderate and similar amounts of diffuse plaques could be found in AD but also control patients. On contrary, dense core plaques were specific of the AD groups and

APP/PS1 and APP-KI NL/G/F mouse models of AD. We performed in-depth analyses of the images, including density and area quantification of the markers, relative colocalization assessment, and mean pixel intensity measurement to address the distribution of APP fragments in AD brains and to provide a thorough molecular characterization of AD as a proteinopathy.

First, we observed in control sections dense staining of APP in neuronal soma of the hippocampus whereas APP staining appeared faint in neuronal soma in AD sections. In the AD hippocampus, APP was prominent in remarkably intense stainings, which appeared as distinct extra-somatic microscopic entities referred to as APP accumulations. The density of APP accumulations was remarkably higher in the hippocampus of patients with FAD, characterized by a much younger age of onset, compared to SAD. Thus, APP accumulations could represent an additional important marker of AD pathology. The quantification of the mean pixel intensity of APP in neuronal soma in the granule cell (GC) or cornu ammonis 3 (CA3) layers showed a large reduction in AD versus control sections. Moreover, an inverse correlation was observed between the burden of APP accumulations in neuropil areas (i.e., surface covered by APP accumulations) and the level of APP expression in neuronal soma, suggesting that APP accumulations might result from a cellular misdistribution.

The topographic organization of APP accumulations in relation to amyloid plaques revealed by antibodies against A β peptide and by congophilic labeling (e.g., using methoxy-X04) unveiled that APP preferentially accumulates in the periphery of dense-core plaques but not around diffuse plaques. The detection of APP around dense-core plaques raises the possibility that some APP fragments also compose amyloid plaques. We characterized the distribution of the APP-Cter and Nter domains within the dense-core plaques labeled with methoxy-X04 and observed that APP-Nter was markedly enriched inside dense-core plaques whereas APP-Cter was absent. Interestingly, BACE1 was found enriched in APP accumulations suggesting that the APP-Nter detected in the core of the plaques is secreted from adjacent sites where APP is cleaved.

We searched for the presence of pre- versus postsynaptic markers, in an effort to clarify the origin of APP accumulations. We did not detect the postsynaptic protein Shank2 or the dendritic protein MAP2 within APP accumulations or dense-core plaques whereas the synaptic vesicle proteins Syt1 and VAMP2 were highly enriched within APP

accumulations. Syntaxin1A, a cell-surface protein present in presynaptic active zones, was also present, but not enriched, within APP accumulations. Extensive analyses of neuritic markers (neurofilaments, tau, myelin basic protein [MBP], p-tau) revealed that APP accumulates together with p-tau, presumably at unmyelinated axons or axon terminals.

Histopathological characterization of the AD mouse models APP/PS1 and APP-KI NL/G/F demonstrated that they both faithfully recapitulate the features of APP accumulations. We took advantage of this correspondence and characterized APP accumulations at the ultrastructural level using EM in APP/PS1 mice. We observed numerous multi-vesicular bodies and autophagic vacuoles in the tissue surrounding the plaques which were abundantly stained for APP-Nter and Cter, suggesting that full-length APP accumulates in membranes of the autophagy lysosomal pathway. Finally, cryosections stained for APP-Cter with DAB and labeled for VAMP2 using immunogold particles, revealed the presence of the presynaptic protein in multi-vesicular bodies positive for APP-Cter suggesting that the multi-vesicular bodies include material deriving from synaptic vesicles containing APP.

3 | DETAILED METHODS AND RESULTS

3.1 | Methods

3.1.1 | Human brain tissue

The use of human brain material (11 control, 12 sporadic AD, and 4 familiar AD with PS1 mutations, see Table 1) was approved by the ethical and research committees after the consent of patients or relatives for research use. Paraffin-embedded samples were obtained from NBB (www.brainbank.nl) or from the KIBB.

3.1.2 | Mice

Heterozygous APP/PS1 female mice co-expressing human APP Swedish mutation (KM670/671NL) and PS1 Δ Exon9⁶⁰ were used in agreement with the Bordeaux/CNRS Animal Care committee. APP-KI

between them, they were more abundant in FAD compared to SAD patients. (C) Close-up images of APP accumulations surrounding an amyloid plaque co-labeled with A β 42 and methoxy-X04. A β 42 and methoxy-X04 colocalize well together but not with APP-Cter. (D) Graph of a Sholl analysis of the number of APP accumulations in function of the distance from the edge of A β 42 plaques. More APP accumulations are present close to the amyloid plaques. (E) Graph of the total area covered by amyloid plaques in the hippocampus of AD cases in function of the total area of APP accumulations. The linear regression of the data presents a positive slope. The Pearson correlation coefficient was 0.79 ($p = 0.011$), indicative of a positive correlation between the amyloid load and the extent of APP accumulations. (F) Scatter plot of MOC between methoxy-X04 and/or APP-Cter and/or A β 42. The analysis revealed a high colocalization between methoxy-X04 and A β 42 but between methoxy-X04 and APP-Cter or between APP-Cter and A β 42 indicating that amyloid plaques and APP accumulations are located nearby but are nonoverlapping. (G) Close-up pictures of hippocampal amyloid plaques labelled with APP-Cter, Nter and methoxy-X04 revealed a remarkable abundance of APP-Nter in the core of dense core amyloid plaques surrounded by APP. (H) Scatter plot of the MOC between methoxy-X04 and APP-Nter or Cter. The analysis revealed a high colocalization between methoxy-X04 and APP-Nter but not with APP-Cter. (I) Scatter plot of the intensity of APP-Cter or Nter labelings within the core of the plaques labeled with methoxy-X04. The data are normalized to the intensity outside the plaques and accumulations represented here by a dashed line. The analysis revealed that APP-Nter is enriched in the core of the plaques whereas APP-Cter is not.

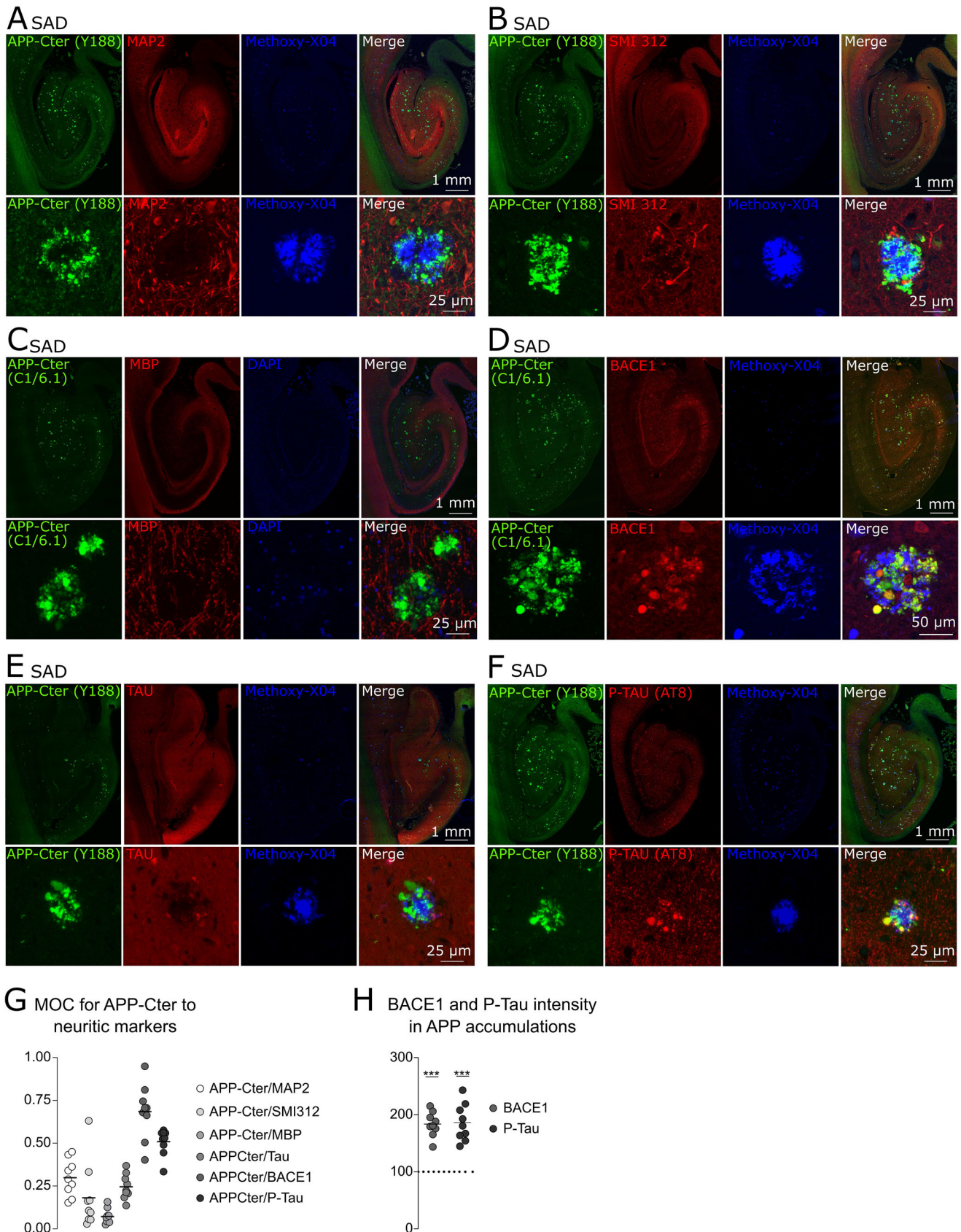


FIGURE 3 Phospho-Tau concentrate in APP accumulations (A) Pictures of a human hippocampal section labeled against APP-Cter and MAP2 and with methoxy-X04. The lower panels show a hippocampal dense-core plaque (revealed by methoxy-X04) and surrounded by APP-Cter. It corresponds to a dark area in the MAP2 channel. (B) Pictures as in (A) but with SMI312. The lower panels show a hippocampal dense-core plaque

TABLE 2 List of antibodies

Antibody	Company	Reference	Antigen retrieval treatment	Species	Dilution
APP-Cter (Y188)	Abcam	32136	Citrate buffer or formic acid 70%	Rabbit	1:500
APP-Cter (C1/6.1)	BioLegend	SIG-39152	Citrate buffer	Mouse	1:500
APP-Nter (JRD32)	Johnson & Johnson	-	Formic acid 70%	Mouse	1:500
APP-Nter (22C11)	eBioscience	14-9749-82	Citrate buffer	Mouse	1:500
BACE1 (D10E5)	Cell Signaling	5606	Citrate buffer	Rabbit	1:500
PS1-CTF (33B10)	N. Robakis laboratory	-	Citrate buffer	Mouse	1:500
A β 42 (12F4)	BioLegend	805501	Formic acid 70%	Mouse	1:500
A β 1-16 (DE2)	Sigma Aldrich	MAB5206	Citrate buffer	Mouse	1:500
MAP2	Sigma Aldrich	M4403	Citrate buffer	Mouse	1:500
MBP	Abcam	ab216668	Citrate buffer	Rabbit	1:500
NeuN	Merck	ABN78	Citrate buffer	Rabbit	1:500
Syntaxin1a	Alomone	ANR-002	Citrate buffer	Rabbit	1:1000
Synaptotagmin1	Synaptic Systems	105011	Citrate buffer	Mouse	1:500
VAMP2	Synaptic Systems	104211	Citrate buffer	Mouse	1:500
Shank2	Synaptic Systems	162 204	Citrate buffer	Guinea pig	1:500

NL-G-F mice expressing the Swedish (KM670/671NL), Iberian (I716F) and Arctic (E693G) mutations⁶¹ were also used.

3.1.3 | List of antibodies

A detailed list of antibodies is available in Table 2.

3.1.4 | Immunohistochemistry on human *post mortem* brain sections

DAB immunostaining

Paraffin-embedded hippocampus sections (5 μ m) were incubated two times in xylene for 10 minutes and hydrated for 3 minutes in different baths ranging from 99% to 70% ethanol concentrations. Then, sections were incubated in a pressure cooker (Biocare Medical) at 110°C for 30 minutes either in citrate buffer (10 mM citric acid [Sigma Aldrich 251275], 0.05% Tween-20 [Sigma Aldrich P7949], pH 6) or formic acid 70% ([Sigma Aldrich F0507], pH 2) depending on the protein staining. Brain sections were washed with phosphate-buffered

saline-Tween 0.05% (PBS-T) and blocked with a peroxidase enzyme blocker for 5 minutes (Dako Dual Endogenous Enzyme Block S2003) and goat serum (NGS; Thermo Fisher Scientific PCN5000) for 20 minutes at room temperature (RT). Sections were incubated at RT for 2 hours with one primary antibody and then with peroxidase-conjugated secondary antibody. Sections were incubated 2 minutes with 3,3'-DAB chromogen solution (Dako EnVision + Dual Link System-HRP [#K4065]). Sections were washed again and incubated with hematoxylin for 5 minutes at RT before being dehydrated in baths of 3 minutes ranging from 70% to 99% ethanol and finally in xylene for 10 minutes. Sections were finally mounted with Vecta mount (VectaMount Permanent Mounting Medium #H-5000) and dried overnight. Preabsorption controls in human sections were performed by using the APP C-terminal peptide sequence KMQQNGYENPTYKFFEQMQN (Proteogenix) at 1 μ g/mL and Y188 or C1/6.1 at 1 μ g/mL (equal mass concentration, i.e., excess molarity of the adsorption peptide).

Immunofluorescence

Brain sections were treated as for the DAB immunostaining. In addition, slices were incubated with an autofluorescence quencher (True-

(revealed by methoxy-X04) and surrounded by APP-Cter. Some SMI312 positive neurites surrounds the plaques but do not colocalize with APP-Cter. (C) Hippocampal sections stained for APP, MBP and DAPI. APP accumulations are mostly found out of regions labelled for MBP. The close-up pictures show the absence of colocalization between MBP and APP. (D) Hippocampal sections stained for APP, BACE1 and methoxy-X04. Close-up pictures show several enlarged neurites positive for BACE1 which colocalizes with APP. (E) Hippocampal sections stained for APP, Tau and methoxy-X04. Close-up pictures show few enlarged neurites positive for Tau and negative for APP. (F) Hippocampal sections stained for APP, phosphorylated-tau (P-Tau) and methoxy-X04. Close-up pictures show several enlarged neurites positive for P-Tau which colocalizes with APP. (G) Scatter plot of the MOC between APP-Cter and the neuritic markers labeled in Fig3. The colocalization is low for MAP2, SMI312, MBP, and Tau but high for BACE1 (0.7) and P-Tau (0.53). (H) Scatter plot of the intensity of P-Tau labeling within APP accumulations. The data are normalized to the intensity outside the APP accumulations represented here by a dashed line. The analysis revealed that BACE1 and P-Tau are enriched inside the APP accumulations

Black Lipofuscin Autofluorescence Quencher–Biotium #23007) for 5 minutes at RT before incubation with secondary antibodies diluted at 1/500 (coupled with Alexa 488 or 568–Thermo Fisher Scientific) and with Methoxy X04 (5 μ M; Tocris Bioscience #4920) or DAPI (300 nM) for 20 minutes. Finally, sections were mounted in Fluoromount™ (Southern Biotech #0100-01) and dried overnight.

3.1.5 | Mouse immunohistochemistry

Mice were first anesthetized by an intraperitoneal injection of pentobarbital (50 mg/kg body weight). Mice were then perfused intracardially with 0.9% NaCl for 1 minute and then with 4% paraformaldehyde in 0.1 mM PBS (PFA 4%) for 4 minutes. Brains were then dissected and post-fixed for 8 hours in PFA 4%. Coronal sections of 50 μ m were cut on a vibratome (Leica VT1200S) and permeabilized in PBS 0.3% Triton X-100 (Sigma Aldrich–#9002-93-1) at RT for 2 hours. The brains of APP-KI NL-G-F mice were paraffin-embedded and cut on microtome into 4 μ m slices.

3.1.6 | Brain section imaging

Brain sections were all imaged using the bright and wide field microscope Nanozoomer 2.0HT (Hamamatsu) with a 20X objective and fixed additional lens 1.75X allowing the acquisition of full sections without mosaicism and a resolution of 454 nm/pixel (55947 DPI). For every experiment, imaging settings and acquisitions were maintained constant between different patient groups.

3.1.7 | Image analysis

Image acquisitions were calibrated and processed as 8-bit grayscale images (0 to 255) using Image J. A high manual threshold was first applied to the APP accumulations and plaques to remove any signal coming from other non-interesting structures. The structures of interest were then saved separately as regions of interest (ROIs) and enlarged by delineating new boundaries 15 μ m away from their detection perimeter for posterior analysis. The two ROIs were then merged and used as an overlay to extract the objects from the initial image. Finally, from the extracted images, colocalization studies were performed between different channels by using the Manders overlap coefficient (MOC) (Figure S1J,K in supporting information). Images were analyzed by using the JACoP plugin (<http://www3.interscience.wiley.com/cgi-bin/fulltext/118727584/PDF> START; 2006), which provides the proportion of co-localized pixels ranging from 0 (no co-localization) to 1 (perfect co-localization). For some markers, the threshold setting was done automatically by using the plugin “Auto threshold,” which provides a set of different automatized algorithms. APP C-terminal accumulations and plaques (methoxy X04) were selected by using the “Max entropy” algorithm that implements the Kapur–Sahoo–Wong thresholding method.⁶² For A β antibody stainings, the algorithm “Yen”

was applied.⁶³ For Syntaxin1a and Shank2 the “Moments” algorithm and for myelin basic protein the “Default” algorithm was applied. Manual thresholding was only applied when none of the automatized algorithms was able to detect reliable markers without a clear signal-to-noise ratio, that is, for APP N-terminal, VAMP2, syt1, BACE1, and PS1. The Costes method was used as a statistical test to evaluate the correlation among different channels.⁶⁴ The *P* value for all the images tested in this study was equal to 1. The average pixel intensity for each of the proteins was also measured within the surface of the APP accumulation and 15 μ m outside using the ROI manager function and the gray value distribution histogram.

DAB stainings were used to count APP accumulations with an automated macro that was segmenting, counting, and measuring the size of each accumulation in different regions of the brain section (https://github.com/fabricecordelieres/IJ-Macro_APP-Plaques-NanoZoomer). Sholl analysis⁶⁵ was used to measure the area and number of APP accumulations around amyloid plaques labeled for A β 42 (https://github.com/fabricecordelieres/IJ-Macro_APP-Aggregates-Per-Plaques-NanoZoomer).

3.1.8 | Electron microscopy–ultrastructure studies

Electron microscopy was performed on samples from the cortex of two wild-type (WT) and three APP/PS1 mice fixed in 2.5% paraformaldehyde/0.1% glutaraldehyde. Brain sections (250 μ m) were permeabilized using sodium borohydride 1% (Sigma Aldrich #452882) at RT for 30 minutes before immunostaining. Brain sections were post-fixed at RT in 1% osmium tetroxide in the dark. Dehydrated slices were incubated into a 50% mix (volume) of Epon 812 resin (Electron Microscopy Sciences) and pure ethanol for 2 hours at RT and finally in pure resin overnight. Slices were finally embedded between two sheets of aclar, and polymerized at 60°C for 48 hours. The ROIs were cut at 500 nm thick sections by using an ultramicrotome and a Diatome diamond knife (Leica EM UC7). Sections of 70 nm thick were then collected on copper grids (Electron Microscopy Sciences) and observed with a transmission electron microscope Hitachi H7650 equipped with a Gatan Orius CCD camera.

3.1.9 | Electron microscopy–Tokuyasu immunolabeling with gold particles

After chemical fixation, small cortical sections were incubated in 2.3 M sucrose overnight at RT. Sections immersed in liquid nitrogen were sliced at 70 nm with a 35° angle Diatome diamond knife at –120°C. After primary immunostaining, sections were incubated with the secondary antibody coupled with gold particles (goat anti-mouse 15 nm with a dilution of 1:50 for VAMP2), and sections were post-fixed with 2% glutaraldehyde. The next wash was done in distilled water and a heavy metal contrast incubation was performed in the dark with aqueous uranyl acetate containing 2% methylcellulose for 10 minutes in ice.

3.1.10 | Statistical analysis

GraphPad Prism 8.0 (GraphPad Software) was used to perform all the statistical analyses. Distribution of the data samples were tested with d'Agostino and Pearson tests. Normally and non-normally distributed data were compared using a two-tailed t-test and Mann-Whitney rank test, respectively. Two-way analysis of variance was used for analysis with two different factors (number of APP accumulations and patient groups). Differences between groups were considered statistically significant when $P < .05$.

3.2 | Results

3.2.1 | Misdistribution of APP in the hippocampus of AD patients

We compared the distribution of APP in the human hippocampus of AD cases versus controls, by collecting paraffin-embedded hippocampal sections from two brain banks: the NBB and the KIBB (see Methods section). Three groups were constituted: 11 control= patients (mean age 79.6 years; 73% F and 27% M), 12 AD patients with the late-onset, sporadic form of the disease (SAD; mean age 81 years; 92% F and 8% M), and 4 patients with the early-onset, familial form (FAD; mean age 48.5 years; 50% F and 50% M; summarized in Table 1; further clinical data tables in Table S1-S3).

We first labeled APP using two specific antibodies against the APP C-terminal domain (APP-Cter): the C1/6.1 antibody and the Y188 antibody (Figure 1A). The sections were imaged with a Nanozoomer 2.0HT slide scanner (Hamamatsu) allowing the acquisition of full sections without mosaicism and a resolution of 454 nm/pixel (55947 DPI). Preadsorption with a recombinant APP-Cter peptide abolished the staining (Figure S1A-B). In control sections, dense DAB staining of APP was observed in neuronal soma of the dentate gyrus GC layer and the pyramidal cell layer in CA4 and CA3 (Figure 1B and C, S1C), whereas APP staining appeared faint in neuronal soma in both FAD and SAD sections (Figure 1B, S1C). In FAD and SAD sections, APP was prominent in remarkably intense stainings, which spread in the different hippocampal regions (Figure 1B, S1C). The intense clusters of APP appeared as distinct extra-somatic microscopic entities (Figure 1C and S1D), which we further refer to as APP accumulations. Of important note, epitopes of the C1/6.1 and Y188 Cter antibodies are distinct from the A β peptide sequence (Figure 1A) and thus the detection of APP accumulations cannot be due to the detection of A β peptides. These accumulations were almost never detected in the hippocampus (Figure 1D, S1E) or in the para-hippocampal cortices of control patients (Figure S1F). Interestingly, whereas they were present in similar amount in the hippocampus and cortex of the SAD group (16 and 14 per mm², respectively), in the FAD group they were significantly more abundant in the hippocampus (65 and 12 per mm², respectively). Moreover, the density of APP accumulations was remarkably higher in the hippocampus of FAD patients compared to SAD (Figure 1D, S1E,F), albeit the Braak and the amyloid stages (Table S1-S3) were comparable between the two AD

groups. In addition, the age of onset of the disease was as expected, lower in the FAD cases than in the SAD cases. Thus, APP accumulations could represent an additional important marker of AD pathology. The size of APP accumulations, which culminates to several thousands of μm^2 , were larger in the CA than in the molecular layer (ML; Figure 1E, S1F).

To provide a molecular characterization of APP accumulations, we developed an immunofluorescence approach to perform triple labeling in human sections (see method and controls in Figure S1G). We first verified the specificity of the two antibodies against APP-Cter by comparing fluorescence intensity in WT versus APP-KO mice. We observed that the C1/6.1 antibody was fully specific showing no labeling in APP-KO mouse brains (Figure S1H). The Y188 antibody was also specific in the gray matter without any neuronal labeling in APP-KO mouse brains (Figure S1I). However, some white matter tracts remained fluorescent in the APP-KO condition revealing that the white matter staining was not specific for APP (Figure S1I, S1C). We then quantitatively ascertained a high colocalization between the two antibodies within APP accumulations (Figure S1J,K). For this, we developed a method based on the subcellular colocalization analysis JACoP,⁶⁶ to calculate the MOC, an indicator of relative colocalization between two channels (Figure S1L,M). The proportion of pixels positive for C1/6.1 labeling that overlapped with pixels positive for Y188 was defined as MOC (C1/6.1/Y188) and was 0.95. The proportion of Y188 pixels overlapping the C1/6.1 pixels was defined as MOC (Y188/C1/6.1) and was 0.74 (Figure S1N). This MOC nomenclature was used in the entire manuscript. There was a considerable enrichment (by a factor 9) of the fluorescent labeling of APP-Cter inside versus outside APP accumulations (Figure S1O).

The observation of accumulations with the APP-Cter antibodies raised the question of whether the APP accumulations also contain the Nter counterpart of APP, which may suggest the presence of full-length APP. To address this question, we labeled the human hippocampal sections with two different antibodies against the Nter domain of APP (Figure 1A), the standard 22C11 antibody and the highly specific JRD32 antibody (Figure S1P). From here, our study was performed on the cohort of samples from the NBB, which contains eight control cases, eight sporadic, and one familial cases (hereafter combined as AD). In control hippocampal sections, the Nter antibodies clearly labeled neuronal soma (Figure 1F and S1Q) as did the Cter antibodies. In AD sections, the Nter antibodies strongly stained APP accumulations detected with Cter labeling (Figure 1F and G and S1Q,R). Nter and Cter antibody labelings displayed a high MOC (Figure 1H and S1S), suggesting that APP accumulations contain full-length APP, albeit the joint presence of APP-Cter and Nter fragments is also possible.

We next investigated whether there was a correlation between the burden of APP accumulations, mostly present within neuropil areas, and a seeming reduction in APP expression in neuronal soma observable in the DAB staining (Figure 1B). Taking advantage of the linearity of the fluorescent signal, we quantified the mean pixel intensity of APP in neuronal soma in the GC or CA3 layers. APP labeling showed a large reduction in AD versus control sections (Figure 1I), in line with the DAB staining observation (Figure 1B). Moreover, an inverse corre-

lation was observed between the burden of APP accumulations in neuropil areas (i.e., surface covered by APP accumulations) and the level of APP expression in neuronal soma, suggesting that APP accumulations might result from a cellular misdistribution (Figure 1J).

3.2.2 | APP accumulations surround dense-core amyloid plaques enriched in APP-Nter

We characterized the topographic organization of APP accumulations in human brain slices in relation to the two main types of plaques, the diffuse plaques revealed with an antibody against the Nter of A β peptides (clone 6E10), and the dense-core plaques,⁶⁷ which can be distinguished by the presence of A β 42 (antibody 12F4) and by congophilic labeling (e.g., using methoxy-X04; Figure 1A). The A β 42 and the A β 1-16 antibodies labeled amyloid plaques in APP/PS1 mice but no staining was observed in WT mice, indicating high specificity for the human A β peptide (Figure S2A-C in supporting information). However, the A β 1-16 antibody being able to also recognize APP, we discriminate between APP and amyloid plaques by combining APP Cter, A β 1-16, and methoxy-X04 labelings. The secondary antibody alone gave no staining (Figure S2C).

In the hippocampus, most amyloid plaques were of the dense-core type (Figure 2A and B), whereas smaller and similar amounts of diffuse plaques could be found in AD but also control patients (Figure 2B). On the contrary, dense core plaques were specific to the AD groups as they were virtually absent in controls. Interestingly, like the APP accumulations, they were more abundant in FAD compared to SAD patients. This observation, together with the spatial proximity between the dense core plaques and the APP accumulations, suggested a connection between them. Indeed, APP accumulations were found in the periphery of dense-core plaques (Figure 2A and C and S2H), which contrasts with their absence around diffuse plaques (Figure S2I-K). Overall, APP accumulations are specific features of the dense-core amyloid plaques, but not of diffuse plaques, which were found in the hippocampus and cortex of AD but also in some non-demented aged humans (Delaère et al.,⁶⁸ Katman et al.,⁶⁹ and Figure S2D-K).

We performed a Sholl analysis⁶⁵ to count the number of APP accumulations at intervals from 5 μ m to 50 μ m away from amyloid plaques (Figure S2L). APP accumulations were found to surround dense-core amyloid plaques, with a progressive decrease away from the plaque's boundaries (Figure 2D). Interestingly, the total area covered by amyloid plaques in the hippocampus is larger in patients exhibiting a larger total area of APP accumulations (Figure 2E) indicating a correlation between the extent of APP accumulations and the amyloid load. Moreover, Bland-Altman analyses of the difference of areas covered by A β 42 and APP accumulations plotted against their average areas revealed that the data sets were of good agreement (Figure S2M). This indicates that APP accumulations and amyloid plaques are probably correlated pathologic features even though they only poorly colocalize (Figure 2F).

The detection of both APP-Cter and -Nter around dense-core plaques raises the possibility that these APP fragments also compose amyloid plaques. We thus characterized the distribution of the APP-Cter and Nter domains within the dense-core plaques. Co-stainings for APP-Nter together with methoxy-X04 unexpectedly revealed a remarkable abundance of APP-Nter in the core of amyloid plaques (Figure 2G and S2N). The colocalization between APP-Nter and the core of the plaques was specific to the Nter domain as the MOC between methoxy-X04 and APP-Nter staining was 0.6 whereas the MOC between methoxy-X04 staining and APP-Cter was only 0.14 (Figure 2H and S2O). APP-Nter was markedly enriched inside dense-core plaques (fluorescent APP-Nter labeling inside amyloid plaques 2.3 times brighter than in the neuropil; Figure 2I). These results suggest that APP-Nter accumulates within the core of the plaques possibly representing another aggregated APP derivative in addition to A β .

3.2.3 | APP accumulations are enriched with presynaptic proteins

Dystrophic neurites of different molecular contents (e.g., expressing neurofilaments or p-tau), have long been reported around amyloid plaques.⁷⁰⁻⁷² In an effort to characterize APP accumulations in relation to these heterogeneous features, we investigated the composition of APP accumulations in neuritic markers. The colocalization of APP accumulations with the dendritic marker MAP2, the phospho-neurofilament (SMI312), the MBP of the myelinated axons, and tau was low in AD conditions (Figure 3A-C,E; Figure S3 in supporting information, control sections). Thus, APP accumulations were distinct from several kinds of dystrophic neurites commonly described around plaques. In addition, BACE1, a protease enriched in axons⁷³ and responsible for the ectodomain shedding of APP which releases the APP-Nter, was found around amyloid plaques as previously reported^{74,75} (Figure 3D). Interestingly, BACE1 displayed a MOC of 0.7 to APP and was enriched within APP accumulations (Figure 3G and H). PS1, the catalytic subunit of γ -secretase, was also found within APP accumulations (Figure S3G,H) with a moderate MOC of APP-Cter to PS1 overlap of 0.4 (Figure S3I) and a modest enrichment of 20% (Figure S3I). The presence of the β - and γ -secretase suggests that APP could be cleaved within accumulations and thus fuel adjacent amyloid plaques in APP-Nter and A β peptides. In contrast to normal tau, p-tau (AT8) was colocalizing with APP (MOC of 0.53) and was enriched within APP accumulations (intensity ratio of 1.86) (Figure 3F-H).

We then searched for the presence of pre- versus postsynaptic markers, in an effort to clarify the origin of APP accumulations. We did not detect the postsynaptic protein Shank 2 within APP accumulations or dense-core plaques (Figure 4A and B and MOCs 4G and S4C in supporting information), whereas a prominent staining of dendrites and spines was observed in both control and AD conditions (Figure 4A). Similarly, the dendritic protein MAP2 was absent from dense-core plaques,⁷⁶ and from APP accumulations. Moreover, the

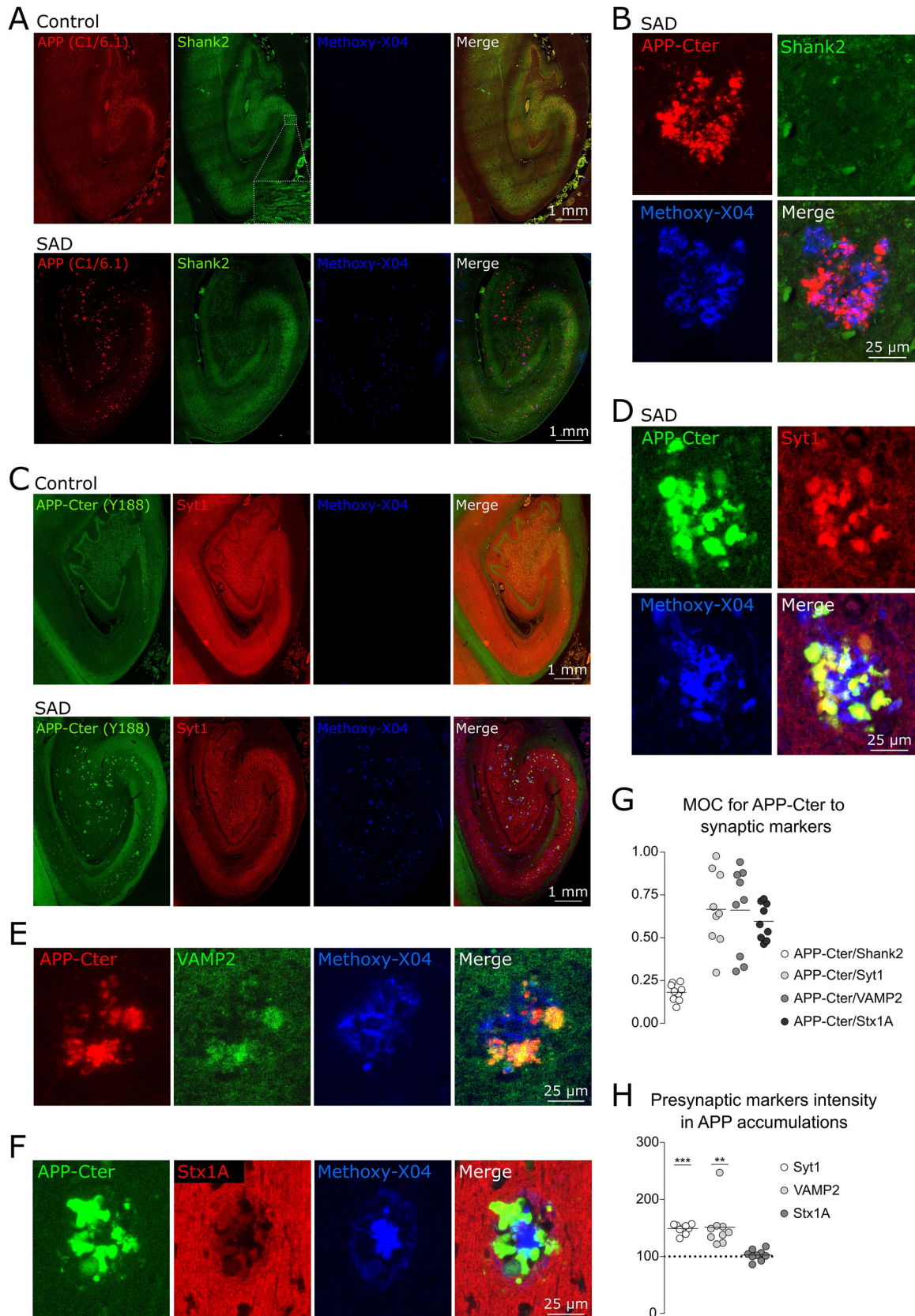


FIGURE 4 Synaptic vesicle proteins but not postsynaptic proteins concentrate within APP accumulations (A) Human hippocampal sections immuno-labeled against APP-Cter and Shank2 and with methoxy-X04. Shank2 is prominently observed in neuronal soma and in the neuropil in both control and AD condition. (B) Close-up pictures of stainings as in 'A' showing the absence of Shank2 in APP accumulations surrounding an amyloid plaque labeled with methoxy-X04. (C) Human hippocampal sections immuno-labeled against APP-Cter and synaptotagmin-1 (Syt1) and with methoxy-X04. In controls, Syt1 is prominently observed in the neuropil, especially in presynaptic terminals in the CA4 region. In AD, Syt1

distinctive lower intensity in MAP2 staining in dense-core plaques and its APP surroundings (Figure 3A), indicates that post-synaptic compartments are not preserved within these hallmarks. Overall, APP does not accumulate together with dendritic or post-synaptic proteins. We then stained for a set of presynaptic proteins (Syt1, VAMP2, and Syntaxin1A) in relation to APP accumulations and amyloid plaques. The three proteins were abundant in the neuropil over the entire hippocampal slice (Figure 4C, S4A,B). Interestingly, the synaptic vesicle proteins Syt1 and VAMP2 were highly enriched within APP accumulations (Figure 4D, E, G, H) whereas they were absent from the core of the plaques (Figure S4C). Syntaxin1A, a cell-surface protein present in presynaptic active zones, was also present, although not enriched, within APP accumulations (Figure 4F–H and S4B).

The observation that APP accumulations contain presynaptic proteins indicates that they may originate from axons or axon terminals. We questioned whether APP accumulations were preferentially segregated in the white matter using MBP staining (Figure 3C and S4D) to delineate white matter tracts. APP mainly accumulated in the gray matter (Figure S4E) and when found in the white matter, the accumulations were significantly smaller (Figure S4F). Collectively, these results indicate that APP and its secretases accumulates together with presynaptic proteins related to vesicle release and p-tau, presumably at presynaptic sites from unmyelinated axons.

3.2.4 | Ultrastructural investigation reveals presynaptic proteins and APP accumulations within multivesicular bodies

To further analyze the APP accumulations, we sought to use AD mouse models. In both APP/PS1⁶⁰ and APP knock-in NL/G/F mice,⁶¹ we observed intense APP accumulations surrounding amyloid plaques (APP/PS1: Figure S5A–S5B in supporting information; Scholl analysis S5C; APP-NL/G/F: S5F–S5G). In addition, as in the human AD brain, the APP accumulations contained the APP-Nter domain (Figure 5A, B; MOCs S5D, E; APP-NL/G/F: S5H,I), displayed a high labeling intensity for Syt1 (Figure 5C) and Vamp2 (Figure S5J), but not for Shank2 (Figure 5D). Of note, AD mouse models present numerous APP accumulations and dense-core plaques in the cortex, contrary to humans for which the APP accumulations were more frequent in the hippocampus.

From a histopathological point of view, both APP/PS1 and APP-KI NL/G/F properly exhibit APP-related AD hallmarks, and faithfully recapitulate the features of APP accumulations. We took advantage

of this correspondence and characterized APP accumulations at the ultrastructural level using EM in APP/PS1 mice. We identified amyloid plaques given their distinctive shapes with radial projections at the micrometric scale^{77,78} (Figure 5E), and their fibrillary structures at the submicrometric scale (Figure S5K). Outside the boundaries of the amyloid plaques (Figure 5E), we frequently observed lysosomes connected to autophagosomes that were highly stained by the DAB reaction associated with either APP-Nter or -Cter antibody (Figure 5F and S5L). We also observed numerous multi-vesicular bodies and autophagic vacuoles all over the tissue surrounding the plaques (Figure 5G, S5M,N), consistent with an impairment of the autophagy–lysosomal pathway currently debated in the AD field.^{79–83}

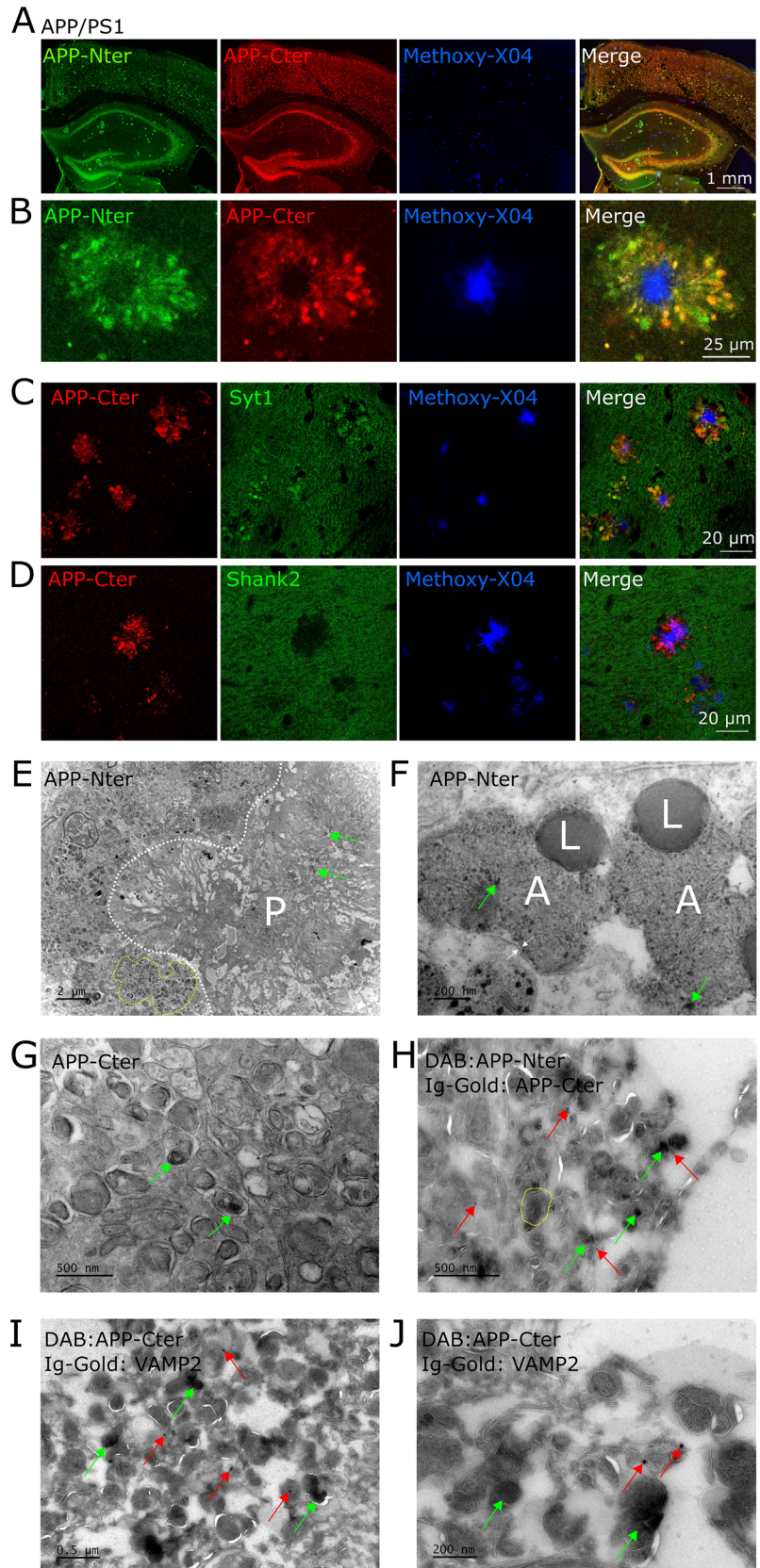
We stained APP-Nter with DAB and labeled APP-Cter using immuno-gold particles on cryosections based on the Tokuyasu method. We observed abundant DAB staining of APP-Nter at the level of membranous accumulations (contrasted in white on dark background in cryosections; Figure 5H, S5O). Importantly, we observed immuno-gold puncta revealing the presence of APP-Cter in the same location as APP-Nter suggesting that full-length APP accumulates in membranes of the autophagy–lysosomal pathway. Finally, cryosections stained for APP-Cter with DAB and labeled for VAMP2 using immuno-gold particles, revealed the presence of the presynaptic protein in multi-vesicular bodies positive for APP-Cter (Figure 5I, J). This suggests that the multi-vesicular bodies derive from misprocessed synaptic vesicles containing APP.

3.2.5 | APP accumulations inversely correlate with neuronal density

We finally evaluated whether APP accumulations participated in the neurodegenerative process by evaluating neuronal loss in their surroundings. We counted NeuN labeled neurons in the somatosensory cortex of APP/PS1 in ROIs containing one, several, or no APP accumulations (Figure 6A). We found an inverse relationship between APP accumulations and neuronal density: The larger the area covered by the APP accumulations was, the fewer neurons were present (Figure 6B). The decrease in neuronal density observed close to APP accumulations was not caused by neuronal dispersion that could have happened due to the surface occupied by the APP accumulations within a finite area but by neuronal loss. Indeed, we counted the number of neurons in the full layer V from the somatosensory cortex or of the full ML of the dentate gyrus in slices from 2-, 5-, and 9-month-old APP/PS1 mice (Figure 6C). In both brain regions, we observed a significant and pro-

strikingly accumulates at the level of APP accumulations. (D) Close-up pictures of stainings as in 'C' showing the presence of Syt1 in APP accumulations close to an amyloid plaque labeled with methoxy-XO4. (E) Close-up pictures of stainings showing the presence of VAMP2 in APP accumulations close to an amyloid plaque labeled with methoxy-XO4 (full-hippocampus acquisition related to this condition are shown in FigS4A). (F) Close-up pictures of stainings showing the presence of syntaxin-1a in APP accumulations nearby an amyloid plaque labeled with methoxy-XO4 (full-hippocampus acquisition related to this condition are shown in FigS4B). (G) Scatter plot of the MOC between APP-Cter and the synaptic markers labeled in Fig4. The colocalization is high for the presynaptic markers Syt1, VAMP2 and Stx1A but low for Shank2. (H) Scatter plot of the intensity of presynaptic markers labelings within APP accumulations. The data are normalized to the intensity outside the APP accumulations represented here by a dashed line. The analysis revealed that synaptic vesicle proteins Syt1 and VAMP2 are enriched inside the APP accumulations whereas the cell surface protein Stx1A is not

FIGURE 5 Electron microscopy analyses reveal presynaptic proteins and APP accumulations within multivesicular bodies (A) APP/PS1 mouse hippocampal sections immuno-labelled against APP-Nter and Cter and with methoxy-X04. (B) Close-up pictures of stainings as in 'A' showing that amyloid plaques are surrounded by APP accumulations as in human AD conditions. (C, D) Close-up pictures of stainings immuno-labelled against APP-Cter and either Syt1 in 'C' or Shank2 in 'D'. (E) Electron microscopy images of a hippocampal section from an APP/PS1 mouse labeled with osmium (membrane marker) and with an antibody against APP-Nter (DAB labeling). An amyloid plaque (P) is marked with DAB (positive for APP-Nter, green arrows) and delimited by a white broken line. Outside the plaque, round membranous organelles, positive for APP-Nter, are abundant. One cluster is highlighted inside a yellow border. (F) Outside the boundaries of amyloid plaques, lysosomes (L) connected to autophagosomes (A) highly stained by the DAB reaction associated with APP-Nter antibody (green arrows) are frequently observed. White arrows point the double membrane. (G) Clusters of multi-vesicular bodies and autophagic vacuoles are observed all over the tissue surrounding the plaques. (H) Cryosections (Tokuyasu method) from an APP/PS1 mouse immuno-labeled against APP-Nter (JRD32; DAB labeling, green arrows) and Cter (Y188; labeled with gold; black dots visible at high magnification, red arrows). The membranes appear finely white on the cryosections. The tissue contains numerous multivesicular bodies; one of them is highlighted inside a yellow border. They are positive for APP-Nter and APP-Cter. (I, J) Hippocampal cryosections immuno-labeled against APP-Cter (DAB labeling, green arrows) and against VAMP2 (immuno-gold; black dots visible at high magnification, red arrows). The tissue contains numerous multivesicular bodies, positive for both APP-Cter and VAMP2



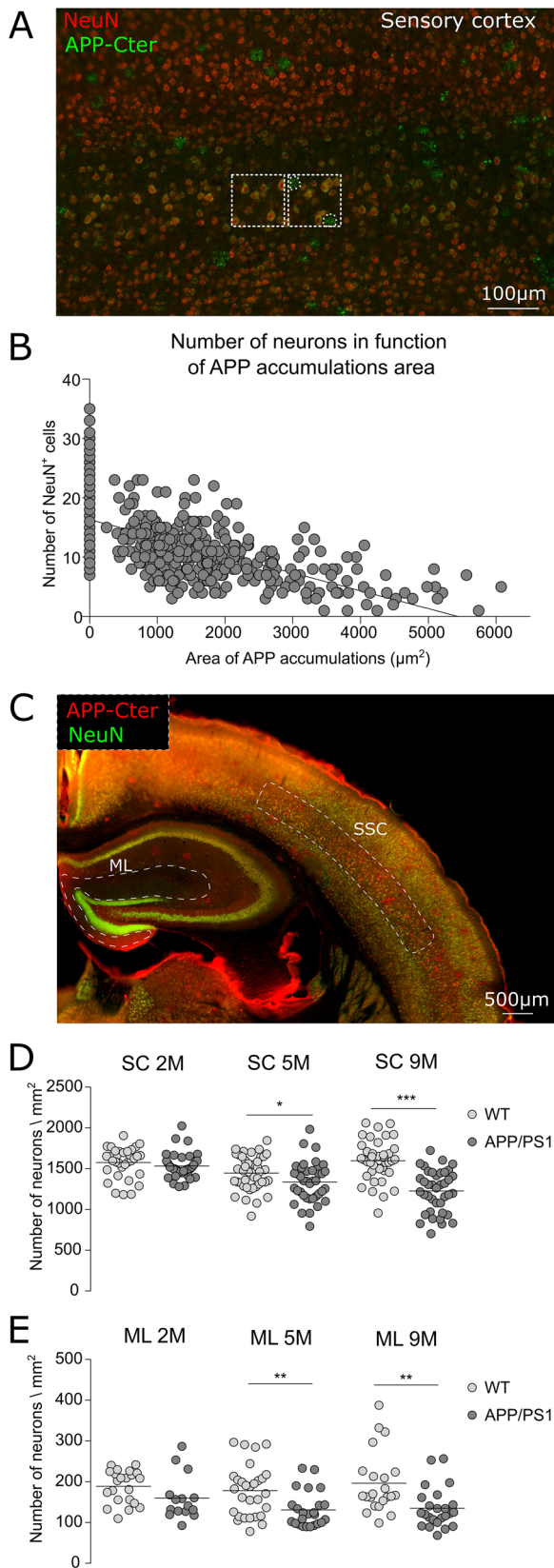


FIGURE 6 The number of APP accumulations inversely correlate with neuronal density (A) Sections of the somatosensory cortex of APP/PS1 immuno-labeled with NeuN and APP-Cter. Using NeuN labelling as a neuronal reporter, we counted neurons in 100 μ m-side squares, used as regions of interest (ROIs). The squares were placed in different regions along the sagittal to temporal axis containing or not

gressive decrease in the number of neurons starting at 5 months in APP/PS1 mice compared to WT (Figure 6D,E). This result suggests a relationship between the number of APP accumulations and neurodegeneration.

ACKNOWLEDGMENTS

We thank Takashi Saito, Takaomi C. Saïdo from RIKEN Brain Institute (Saitama, Japan), and Per Nilsson (Karolinska Institute, Stockholm) for the gift of APP-NL/G/F brain slices. The *post mortem* human brain tissue for this study was supplied by the Netherlands Brain Bank (Amsterdam, the Netherlands) and the Karolinska Institute Brain Bank (Stockholm, Sweden); we thank all the donors for the tissue used in this study. We thank Caroline Graff from the Karolinska Institute Brain Bank. We thank Juan Pita-Almenar from Janssen Pharmaceutica for the gift of JRD32 antibody. Imaging was performed at the Bordeaux Imaging Center, a service unit of the CNRS-INSERM and Bordeaux University, member of the national infrastructure France BioImaging (ANR-10-INBS-04). This project was supported by the CNRS, it has received funding from the European Union's Horizon 2020 research and innovation program under grant agreement No. 676144, from the foundation Plan Alzheimer, from France Alzheimer, and from the Fondation pour la Recherche Médicale (project #DEQ20160334900).

CONFLICTS OF INTEREST

The authors declare that they have no conflicts of interest.

AUTHOR CONTRIBUTIONS

Tomas Jorda-Siquier, Melina Petrel, and Vladimir Kouskoff conducted the experiments; Fabrice Cordelieres developed ImageJ macros for images analyses; Susanne Frykman supervised the experiments performed at the Karolinska Institute; Una Smalovic and Ulrike Muller provided research materials and advice; Tomas Jorda-Siquier and Gael Barthe designed the experiments; Tomas Jorda-Siquier, Christophe Mulle, and Gael Barthe wrote the article.

ORCID

Gaël Barthe  <https://orcid.org/0000-0003-4025-1616>

REFERENCES

- De Strooper B, Saftig P, Craessaerts K, et al. Deficiency of presenilin-1 inhibits the normal cleavage of amyloid precursor protein. *Nature*. 1998;391:387-390.

one or several APP accumulations. (B) Analyses of pictures as in 'A' revealed an inverse relationship between the area covered by APP accumulations and neuronal density within the ROIs, the larger the area covered by the APP accumulations, the fewer neurons were present. (C) Pictures of APP/PS1 brain sections immuno-labeled with NeuN and APP-Cter. ROIs of the whole hippocampal molecular layer (ML) area and of the somatosensory cortex (SSC) where numbers of neurons were counted (results in 'D' and 'E') are highlighted by dashed lines. (D, E) Analyses of pictures as in 'C' revealed a neuronal loss in APP/PS1 at both 5 and 9 months-old in SC and in ML. The WT littermates do not present any neuronal loss

2. Goate A, Chartier-Harlin MC, Mullan M, et al. Segregation of a missense mutation in the amyloid precursor protein gene with familial Alzheimer's disease. *Nature*. 1991;349:704-706.
3. Sherrington R, Rogaev EI, Liang Y, et al. Cloning of a gene bearing missense mutations in early-onset familial Alzheimer's disease. *Nature*. 1995;375:754-760.
4. Hardy JA, Higgins GA. Alzheimer's disease: the amyloid cascade hypothesis. *Science*. 1992;256:184-185.
5. Huang L-K, Chao S-P, Hu C-J. Clinical trials of new drugs for Alzheimer disease. *J Biomed Sci*. 2020;27:18.
6. Mangialasche F, Solomon A, Winblad B, Mecocci P, Kivipelto M. Alzheimer's disease: clinical trials and drug development. *Lancet Neurol*. 2010;9:702-716.
7. Kuller LH, Lopez OL. ENGAGE and EMERGE: truth and consequences? *Alzheimers Dement*. 2021;17:692-695.
8. Ross CA, Poirier MA. Protein aggregation and neurodegenerative disease. *Nat Med*. 2004;10:S10-S17.
9. Soto C, Pritzkow S. Protein misfolding, aggregation, and conformational strains in neurodegenerative diseases. *Nat Neurosci*. 2018;21:1332-1340.
10. Glenner GG, Wong CW. Alzheimer's disease and Down's syndrome: sharing of a unique cerebrovascular amyloid fibril protein. *Biochem Biophys Res Commun*. 1984;122:1131-1135.
11. Lemere CA, Blusztajn JK, Yamaguchi H, Wisniewski T, Saido TC, Selkoe DJ. Sequence of deposition of heterogeneous amyloid beta-peptides and APO E in Down syndrome: implications for initial events in amyloid plaque formation. *Neurobiol Dis*. 1996;3:16-32.
12. Mann DM. Alzheimer's disease and Down's syndrome. *Histopathology*. 1988;13:125-137.
13. Rovelet-Lecrux A, Hannequin D, Raux G, et al. APP locus duplication causes autosomal dominant early-onset Alzheimer disease with cerebral amyloid angiopathy. *Nat Genet*. 2006;38:24-26.
14. Sleegers K, Brouwers N, Gijselincx I, et al. APP duplication is sufficient to cause early onset Alzheimer's dementia with cerebral amyloid angiopathy. *Brain*. 2006;129:2977-2983.
15. Huang Y-WA, Zhou B, Wernig M, Südhof TC. ApoE2, ApoE3, and ApoE4 differentially stimulate APP transcription and A β secretion. *Cell*. 2017;168:427-441.e21
16. Bentahir M, Nyabi O, Verhamme J, et al. Presenilin clinical mutations can affect gamma-secretase activity by different mechanisms. *J Neurochem*. 2006;96:732-742.
17. Cacquevel M, Aeschbach L, Houacine J, Fraering PC. Alzheimer's disease-linked mutations in presenilin-1 result in a drastic loss of activity in purified γ -secretase complexes. *PLoS One*. 2012;7:e35133.
18. Sun L, Zhou R, Yang G, Shi Y. Analysis of 138 pathogenic mutations in presenilin-1 on the in vitro production of A β 42 and A β 40 peptides by γ -secretase. *Proc Natl Acad Sci USA*. 2017;114:E476-E485.
19. Woodruff G, Young JE, Martinez FJ, et al. The presenilin-1 Δ E9 mutation results in reduced γ -secretase activity, but not total loss of PS1 function, in isogenic human stem cells. *Cell Rep*. 2013;5:974-985.
20. Barthelet G, Shioi J, Shao Z, Ren Y, Georgakopoulos A, Robakis NK. Inhibitors of γ -secretase stabilize the complex and differentially affect processing of amyloid precursor protein and other substrates. *FASEB J*. 2011;25:2937-2946.
21. Barthelet G, Georgakopoulos A, Robakis NK. Cellular mechanisms of γ -secretase substrate selection, processing and toxicity. *Prog Neurobiol*. 2012;98:166-175.
22. Deyts C, Clutter M, Herrera S, Jovanovic N, Goddi A, Parent AT. Loss of presenilin function is associated with a selective gain of APP function. *Elife*. 2016;5:e15645.
23. Jiang Y, Mullaney KA, Peterhoff CM, et al. Alzheimer's-related endosome dysfunction in Down syndrome is A β -independent but requires APP and is reversed by BACE-1 inhibition. *Proc Natl Acad Sci USA*. 2010;107:1630-1635.
24. Checler F, Afram E, Pardossi-Piquard R, Lauritzen I. Is γ -secretase a beneficial inactivating enzyme of the toxic APP C-terminal fragment C99? *J Biol Chem*. 2021;296:100489.
25. DeKosky ST, Scheff SW. Synapse loss in frontal cortex biopsies in Alzheimer's disease: correlation with cognitive severity. *Ann Neurol*. 1990;27:457-464.
26. Scheff SW, Price DA, Schmitt FA, DeKosky ST, Mufson EJ. Synaptic alterations in CA1 in mild Alzheimer disease and mild cognitive impairment. *Neurology*. 2007;68:1501-1508.
27. Selkoe DJ. Alzheimer's disease is a synaptic failure. *Science*. 2002;298:789-791.
28. Terry RD, Masliah E, Salmon DP, et al. Physical basis of cognitive alterations in Alzheimer's disease: synapse loss is the major correlate of cognitive impairment. *Ann Neurol*. 1991;30:572-580.
29. Barthelet G, Jordà-Siquier T, Rumi-Masante J, Bernadou F, Müller U, Mülle C. Presenilin-mediated cleavage of APP regulates synaptotagmin-7 and presynaptic plasticity. *Nat Commun*. 2018;9:4780.
30. Haytural H, Jordà-Siquier T, Winblad B, et al. Distinctive alteration of presynaptic proteins in the outer molecular layer of the dentate gyrus in Alzheimer's disease. *Brain Commun*. 2021;3:fcab079.
31. Haytural H, Mermelekas G, Emre C, et al. The proteome of the dentate terminal zone of the perforant path indicates presynaptic impairment in Alzheimer disease. *Mol Cell Proteomics*. 2020;19:128-141.
32. de Wilde MC, Overk CR, Sijben JW, Masliah E. Meta-analysis of synaptic pathology in Alzheimer's disease reveals selective molecular vesicular machinery vulnerability. *Alzheimers Dement*. 2016;12:633-644.
33. Honer WG, Barr AM, Sawada K, et al. Cognitive reserve, presynaptic proteins and dementia in the elderly. *Transl Psychiatry*. 2012;2:e114.
34. Yu L, Tasaki S, Schneider JA, et al. Cortical proteins associated with cognitive resilience in community-dwelling older persons. *JAMA Psychiatry*. 2020;77(11):1172-1180.
35. Barthelet G, Mülle C. Presynaptic failure in Alzheimer's disease. *Prog Neurobiol*. 2020;194:101801.
36. Arai H, Lee VM, Otvos L, et al. Defined neurofilament, tau, and beta-amyloid precursor protein epitopes distinguish Alzheimer from non-Alzheimer senile plaques. *Proc Natl Acad Sci*. 1990;87:2249-2253.
37. Cummings BJ, Su JH, Geddes JW, et al. Aggregation of the amyloid precursor protein within degenerating neurons and dystrophic neurites in Alzheimer's disease. *Neuroscience*. 1992;48:763-777.
38. Eisele YS, Obermüller U, Heilbronner G, et al. Peripherally applied A β -containing inoculates induce cerebral beta-amyloidosis. *Science*. 2010;330:980-982.
39. Meyer-Luehmann M, Coomaraswamy J, Bolmont T, et al. Exogenous induction of cerebral beta-amyloidogenesis is governed by agent and host. *Science*. 2006;313:1781-1784.
40. Motter R, Vigo-Pelfrey C, Kholodenko D, et al. Reduction of beta-amyloid peptide42 in the cerebrospinal fluid of patients with Alzheimer's disease. *Ann Neurol*. 1995;38:643-648.
41. Gouras GK, Almeida CG, Takahashi RH. Intraneuronal abeta accumulation and origin of plaques in Alzheimer's disease. *Neurobiol Aging*. 2005;26:1235-1244.
42. Kohli BM, Pflieger D, Mueller LN, et al. Interactome of the amyloid precursor protein APP in brain reveals a protein network involved in synaptic vesicle turnover and a close association with Synaptotagmin-1. *J Proteome Res*. 2012;11:4075-4090.
43. Heeroma JH, Roelandse M, Wierda K, et al. Trophic support delays but does not prevent cell-intrinsic degeneration of neurons deficient for munc18-1. *Eur J Neurosci*. 2004;20:623-634.
44. Fernández-Chacón R, Wölfel M, Nishimune H, et al. The synaptic vesicle protein CSP alpha prevents presynaptic degeneration. *Neuron*. 2004;42:237-251.
45. Sharma M, Burré J, Bronk P, Zhang Y, Xu W, Südhof TC. CSP α knock-out causes neurodegeneration by impairing SNAP-25 function. *EMBO J*. 2012;31:829-841.

46. Peng L, Liu H, Ruan H, et al. Cytotoxicity of botulinum neurotoxins reveals a direct role of syntaxin 1 and SNAP-25 in neuron survival. *Nat Commun*. 2013;4:1472.
47. Ferguson B, Matyszak MK, Esiri MM, Perry VH. Axonal damage in acute multiple sclerosis lesions. *Brain*. 1997;120(Pt 3):393-399.
48. Kuhlmann T, Lingfeld G, Bitsch A, Schuchardt J, Brück W. Acute axonal damage in multiple sclerosis is most extensive in early disease stages and decreases over time. *Brain*. 2002;125:2202-2212.
49. Umehara F, Abe M, Koreeda Y, Izumo S, Osame M. Axonal damage revealed by accumulation of beta-amyloid precursor protein in HTLV-I-associated myelopathy. *J Neurol Sci*. 2000;176:95-101.
50. Mori I, Goshima F, Mizuno T, et al. Axonal injury in experimental herpes simplex encephalitis. *Brain Res*. 2005;1057:186-190.
51. Gentleman SM, Nash MJ, Sweeting CJ, Graham DI, Roberts GW. Beta-amyloid precursor protein (beta APP) as a marker for axonal injury after head injury. *Neurosci Lett*. 1993;160:139-144.
52. Rorke-Adams LB. 45-Neuropathology of abusive head trauma. In: Jenny C, ed. *Child Abuse and Neglect*. Philadelphia: W.B. Saunders; 2011:413-428.
53. Koo EH, Sisodia SS, Archer DR, et al. Precursor of amyloid protein in Alzheimer disease undergoes fast anterograde axonal transport. *Proc Natl Acad Sci USA*. 1990;87:1561-1565.
54. Gunawardena S, Yang G, Goldstein LSB. Presenilin controls kinesin-1 and dynein function during APP-vesicle transport in vivo. *Hum Mol Genet*. 2013;22:3828-3843.
55. Weingarten MD, Lockwood AH, Hwo SY, Kirschner MW. A protein factor essential for microtubule assembly. *Proc Natl Acad Sci USA*. 1975;72:1858-1862.
56. Peters F, Salihoglu H, Pratsch K, et al. Tau deletion reduces plaque-associated BACE1 accumulation and decelerates plaque formation in a mouse model of Alzheimer's disease. *EMBO J*. 2019;38:e102345.
57. Barthet G, Mulle C. Presynaptic failure in Alzheimer's disease. *Prog Neurobiol*. 2020;194:101801.
58. Knopman DS, Jones DT, Greicius MD. Failure to demonstrate efficacy of aducanumab: an analysis of the EMERGE and ENGAGE trials as reported by Biogen, December 2019. *Alzheimers Dement*. 2021;17:696-701.
59. Peters F, Salihoglu H, Rodrigues E, et al. BACE1 inhibition more effectively suppresses initiation than progression of β -amyloid pathology. *Acta Neuropathol*. 2018;135:695-710.
60. Jankowsky JL, Fadale DJ, Anderson J, et al. Mutant presenilins specifically elevate the levels of the 42 residue beta-amyloid peptide in vivo: evidence for augmentation of a 42-specific gamma secretase. *Hum Mol Genet*. 2004;13:159-170.
61. Saito T, Matsuba Y, Mihira N, et al. Single app knock-in mouse models of Alzheimer's disease. *Nat Neurosci*. 2014;17:661-663.
62. Kapur JN, Sahoo PK, Wong AKC. A new method for gray-level picture thresholding using the entropy of the histogram. *Comput Vision Gr Image Process*. 1985;29:273-285.
63. Yen JC, Chang FJ, Chang S. A new criterion for automatic multilevel thresholding. *IEEE Trans Image Process*. 1995;4:370-378.
64. Dunn KW, Kamocka MM, McDonald JH. A practical guide to evaluating colocalization in biological microscopy. *Am J Physiol Cell Physiol*. 2011;300:C723-742.
65. Sholl DA. Dendritic organization in the neurons of the visual and motor cortices of the cat. *J Anat*. 1953;87:387-406.
66. Bolte S, Cordelières FP. A guided tour into subcellular colocalization analysis in light microscopy. *J Microsc*. 2006;224:213-232.
67. Mesulam MM, Geula C. Butyrylcholinesterase reactivity differentiates the amyloid plaques of aging from those of dementia. *Ann Neurol*. 1994;36:722-727.
68. Delaère P, He Y, Fayet G, Duyckaerts C, Haww JJ. Beta A4 deposits are constant in the brain of the oldest old: an immunocytochemical study of 20 French centenarians. *Neurobiol Aging*. 1993;14:191-194.
69. Katzman R, Terry R, DeTeresa R, et al. Clinical, pathological, and neurochemical changes in dementia: a subgroup with preserved mental status and numerous neocortical plaques. *Ann Neurol*. 1988;23:138-144.
70. Masliah E, Mallory M, Hansen L, Alford M, DeTeresa R, Terry R. An antibody against phosphorylated neurofilaments identifies a subset of damaged association axons in Alzheimer's disease. *Am J Pathol*. 1993;142:871-882.
71. Sharoar MG, Hu X, Ma X-M, Zhu X, Yan R. Sequential formation of different layers of dystrophic neurites in Alzheimer's brains. *Mol Psychiatry*. 2019;24:1369-1382.
72. Su JH, Cummings BJ, Cotman CW. Early phosphorylation of tau in Alzheimer's disease occurs at Ser-202 and is preferentially located within neurites. *Neuroreport*. 1994;5:2358-2362.
73. Laird FM, Cai H, Savonenko AV, et al. BACE1, a major determinant of selective vulnerability of the brain to amyloid-beta amyloidogenesis, is essential for cognitive, emotional, and synaptic functions. *J Neurosci*. 2005;25:11693-11709.
74. Zhang X-M, Cai Y, Xiong K, et al. Beta-secretase-1 elevation in transgenic mouse models of Alzheimer's disease is associated with synaptic/axonal pathology and amyloidogenesis: implications for neuritic plaque development. *Eur J Neurosci*. 2009;30:2271-2283.
75. Kandalepas PC, Sadleir KR, Eimer WA, Zhao J, Nicholson DA, Vassar R. The Alzheimer's β -secretase BACE1 localizes to normal presynaptic terminals and to dystrophic presynaptic terminals surrounding amyloid plaques. *Acta Neuropathol*. 2013;126:329-352.
76. D'Andrea MR, Nagele RG. MAP-2 immunolabeling can distinguish diffuse from dense-core amyloid plaques in brains with Alzheimer's disease. *Biotech Histochem*. 2002;77:95-103.
77. Wisniewski HM, Wegiel J, Wang KC, Kujawa M, Lach B. Ultrastructural studies of the cells forming amyloid fibers in classical plaques. *Can J Neurol Sci*. 1989;16:535-542.
78. Narang HK. High-resolution electron microscopic analysis of the amyloid fibril in Alzheimer's disease. *J Neuropathol Exp Neurol*. 1980;39:621-631.
79. Nixon RA, Wegiel J, Kumar A, et al. Extensive involvement of autophagy in Alzheimer disease: an immuno-electron microscopy study. *J Neuropathol Exp Neurol*. 2005;64:113-122.
80. Sanchez-Varo R, Trujillo-Estrada L, Sanchez-Mejias E, et al. Abnormal accumulation of autophagic vesicles correlates with axonal and synaptic pathology in young Alzheimer's mice hippocampus. *Acta Neuropathol*. 2012;123:53-70.
81. Lee J-H, Yu WH, Kumar A, et al. Lysosomal proteolysis and autophagy require presenilin 1 and are disrupted by Alzheimer-related PS1 mutations. *Cell*. 2010;141:1146-1158.
82. Neely KM, Green KN, LaFerla FM. Presenilin is necessary for efficient proteolysis through the autophagy-lysosome system in a γ -secretase-independent manner. *J Neurosci*. 2011;31:2781-2791.
83. Zhang X, Garbett K, Veeraraghavalu K, et al. A role for presenilins in autophagy revisited: normal acidification of lysosomes in cells lacking PSEN1 and PSEN2. *J Neurosci*. 2012;32:8633-8648.

SUPPORTING INFORMATION

Additional supporting information may be found in the online version of the article at the publisher's website.

How to cite this article: Jordà-Siquier T, Petrel M, Kouskoff V, et al. APP accumulates with presynaptic proteins around amyloid plaques: A role for presynaptic mechanisms in Alzheimer's disease? *Alzheimer's Dement*. 2022;18:2099-2116. <https://doi.org/10.1002/alz.12546>